

Figure 1: Model architecture of the proposed generative model for the Bayesian latent causal discovery task to learn latent SCM from low-level data.

- We propose a general algorithm for Bayesian causal discovery in the latent space of a generative model, learning a distribution over causal variables, structure and parameters in linear Gaussian latent SCMs with random, known interventions. Figure 1 illustrates an overview of the proposed method.
- By learning the structure and parameters of a latent SCM, we implicitly induce a joint distribution over the causal variables. Hence, sampling from this distribution is equivalent to ancestral sampling through the latent SCM. As such, we address a challenging, simultaneous optimization problem that is often encountered during causal discovery in latent space: one cannot find the right graph without the right causal variables, and vice versa.
- On a synthetically generated dataset and an image dataset used to benchmark causal model performance (Ke et al., 2021), we evaluate our method along three axes – uncovering causal variables, structure, and parameters – consistently outperforming baselines. We demonstrate its ability to perform image generation from unseen interventional distributions.

2 PRELIMINARIES

2.1 STRUCTURAL CAUSAL MODELS

A Structural Causal Model (SCM) is defined by a set of equations which represent the mechanisms by which each endogenous variable z_i depends on its direct causes $z_{pa(i)}^{\mathcal{G}}$ and a corresponding exogenous noise variable ϵ_i . The direct causes are subsets of other endogenous variables. If the causal parent assignment is assumed to be acyclic, then an SCM is associated with a Directed Acyclic Graph (DAG) $\mathcal{G} = (V, E)$, where V corresponds to the endogenous variables and E encodes direct cause-effect relationships. The exact value taken on by a causal variable z_i , is given by local causal mechanisms f_i conditional on $z_{pa(i)}^{\mathcal{G}}$, the parameters Θ_i , and the node’s noise variable ϵ_i , as given in equation 1. For linear Gaussian additive noise SCMs with equal noise variance, i.e., the setting that we focus on in this work, all f_i ’s are linear functions, and Θ denotes the weighted adjacency matrix W , where each W_{ji} is the edge weight from $j \rightarrow i$. The linear Gaussian additive noise SCM thus reduces to equation 2,

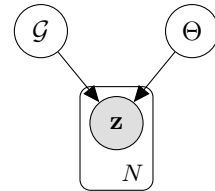


Figure 2: BN for prior works in causal discovery and structure learning

$$z_i = f_i(z_{pa(i)}^{\mathcal{G}}, \Theta, \epsilon_i), \quad (1) \quad z_i = \sum_{j \in pa_{\mathcal{G}}(i)} W_{ji} \cdot z_j + \epsilon_i. \quad (2)$$

2.2 CAUSAL DISCOVERY

Structure learning in prior work refers to learning a DAG according to some optimization criterion with or without the notion of causality (e.g., He et al. (2019)). The task of causal discovery on the other hand, is more specific in that it refers to learning the structure (also parameters, in some cases) of SCMs, and subscribes to causality and interventions like that of Pearl (2009). That is, the methods aim to estimate (\mathcal{G}, Θ) . These approaches often resort to modular likelihood scores over causal variables – like the BGe score (Geiger and Heckerman, 1994; Kuipers et al., 2022) and BDe score (Heckerman et al., 1995) – to learn the right structure. However, these methods all assume a dataset of observed causal variables. These approaches either obtain a maximum likelihood estimate,

$$\mathcal{G}^* = \arg \max_{\mathcal{G}} p(Z | \mathcal{G}) \quad \text{or} \quad (\mathcal{G}^*, \Theta^*) = \arg \max_{\mathcal{G}, \Theta} p(Z | \mathcal{G}, \Theta), \quad (3)$$

or in the case of Bayesian causal discovery (Heckerman et al., 1997), variational inference is typically used to approximate a joint posterior distribution $q_{\phi}(\mathcal{G}, \Theta)$ to the true posterior $p(\mathcal{G}, \Theta | Z)$ by minimizing the KL divergence between the two,

$$D_{\text{KL}}(q_{\phi}(\mathcal{G}, \Theta) || p(\mathcal{G}, \Theta | Z)) = -\mathbb{E}_{(\mathcal{G}, \Theta) \sim q_{\phi}} \left[\log p(Z | \mathcal{G}, \Theta) - \log \frac{q_{\phi}(\mathcal{G}, \Theta)}{p(\mathcal{G}, \Theta)} \right], \quad (4)$$

where $p(\mathcal{G}, \Theta)$ is a prior over the structure and parameters of the SCM – possibly encoding DAGness, sparse connections, or low-magnitude edge weights. Figure 2 shows the Bayesian Network (BN) over which inference is performed for causal discovery tasks.

2.3 LATENT CAUSAL DISCOVERY

In more realistic scenarios, the learner does not directly observe causal variables and they must be learned from low-level data. The causal variables, structure, and parameters are part of a latent SCM. The goal of causal representation learning models is to perform inference of, and generation from, the true latent SCM. Yang et al. (2021) proposes a Causal VAE but is in a supervised setup where one has labels on causal variables and the focus is on disentanglement. Kocaoglu et al. (2017) present causal generative models trained in an adversarial manner but assumes observations of causal variables. Given the right causal structure as a prior, the work focuses on generation from conditional and interventional distributions.

In both the causal representation learning and causal generative model scenarios mentioned above, the Ground Truth (GT) causal graph and parameters of the latent SCM are arbitrarily defined on real datasets and the setting is supervised. Contrary to this, our setting is unsupervised and we are interested in recovering the GT underlying SCM and causal variables that generate the low-level observed data – we define this as the problem of *latent causal discovery*, and the BN over which we want to perform inference on is given in figure 3. In the upcoming sections, we discuss related work, formulate our problem setup and propose an algorithm for Bayesian latent causal discovery, evaluate with experiments on causally created vector data and image data, and perform sampling from unseen interventional image distributions to showcase generalization of learned latent SCMs.

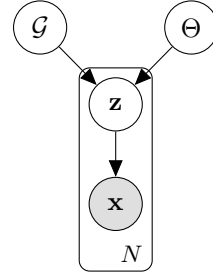


Figure 3: BN for the latent causal discovery task that generalizes standard causal discovery setups

3 RELATED WORK

Prior work can be classified into Bayesian (Koivisto and Sood, 2004; Heckerman et al., 2006; Friedman and Koller, 2013) or maximum likelihood (Brouillard et al., 2020; Wei et al., 2020; Ng et al., 2022) methods, that learn the structure and parameters of SCMs using either score-based (Kass and Raftery, 1995; Barron et al., 1998; Heckerman et al., 1995) or constraint-based (Cheng et al., 2002; Lehmann and Romano, 2005) approaches.

Causal discovery and structure learning: Work in this category assume causal variables are observed and do not operate on low-level data (Spirtes et al., 2000; Viinikka et al., 2020; Yu et al.,

2021; Zhang et al., 2022). Peters and Bühlmann (2014) prove identifiability of linear Gaussian SCMs with equal noise variances. Bengio et al. (2019) use the speed of adaptation as a signal to learn the causal direction. Ke et al. (2019) explore learning causal models from unknown, while Scherrer et al. (2021); Tigas et al. (2022); Agrawal et al. (2019); Toth et al. (2022) focus on active learning and experimental design setups on how to perform interventions to efficiently learn causal models. Transformer (Vaswani et al., 2017) based approach learns structure from synthetic datasets and generalize to naturalistic graphs (Ke et al., 2022). Zheng et al. (2018) introduce an acyclicity constraint that penalizes cyclic graphs, thereby restricting search close to the DAG space. Lachapelle et al. (2019) leverages this constraint to learn DAGs in nonlinear SCMs. Pamfil et al. (2020); Lippe et al. (2022) perform structure learning on temporal data.

Latent variable models with predefined structure: Examples include VAE (Kingma and Welling, 2013; Rezende et al., 2014) which has an independence assumption between latent variables. To overcome this, Sønderby et al. (2016) and Zhao et al. (2017) define latent variables with a chain structure in VAEs. Kingma et al. (2016) uses inverse autoregressive flows to improve upon the diagonal covariance of latent variables in VAEs.

Latent variable models with learned structure: GraphVAE (He et al., 2019) learns the edges between latent variables without incorporating notions of causality. Brehmer et al. (2022) present identifiability theory for learning causal representations and propose a practical algorithm for this under the assumption of having access to pairs of observational and interventional data.

Supervised causal representation learning: Kocaoglu et al. (2017); Shen et al. (2020); Moraffah et al. (2020) introduce generative models that use an SCM-based prior in latent space. In Shen et al. (2020), the goal is to learn causally disentangled variables. Yang et al. (2021) learn a DAG on CelebA and a causally generated pendulum image dataset but assume complete access to the causal variables. Lopez-Paz et al. (2016) establishes observable causal footprints in images.

4 LEARNING LATENT SCMS FROM LOW-LEVEL DATA

4.1 PROBLEM SCENARIO

We are given a dataset $\mathcal{D} = \{\mathbf{x}^{(1)}, \dots, \mathbf{x}^{(N)}\}$, where each $\mathbf{x}^{(i)}$ is a high-dimensional observed data – for simplicity, we assume $\mathbf{x}^{(i)}$ is a vector in \mathbb{R}^D but the setup extends to other inputs as well (like images, as we will see in the next section). We assume that there exist latent variables $\mathbf{Z} = \{\mathbf{z}^{(i)} \in \mathbb{R}^d\}_{i=1}^N$ with $d \leq D$, that explain the data, and these latent variables have an SCM with structure \mathcal{G}_{GT} and parameters Θ_{GT} associated with them. We wish to invert the data generation process $g : (\mathbf{Z}, \mathcal{G}, \Theta) \rightarrow \mathcal{D}$ where the causal variables \mathbf{Z} are in the latent space. In the setting, we also have access to the intervention targets $\mathcal{I} = \{\mathcal{I}^{(i)}\}_{i=1}^N$ where each $\mathcal{I}^{(i)} \in \{0, 1\}^d$. The j^{th} dimension of $\mathcal{I}^{(i)}$ takes a value of 1 if node j was intervened on in data sample i , and 0 otherwise.

4.2 GENERAL METHOD

We aim to obtain a posterior estimate over the entire latent SCM, $p(\mathbf{Z}, \mathcal{G}, \Theta \mid \mathcal{D})$. Computing the true posterior analytically requires calculating the marginal likelihood $p(\mathcal{D})$ which gets quickly intractable due to the number of possible DAGs growing super-exponentially with respect to the number of nodes. Thus, we resort to variational inference (Blei et al., 2017) that provides a tractable way to learn an approximate posterior $q_\phi(\mathbf{Z}, \mathcal{G}, \Theta)$ with variational parameters ϕ , close to the true posterior $p(\mathbf{Z}, \mathcal{G}, \Theta \mid \mathcal{D})$ by maximizing the Evidence Lower Bound (ELBO),

$$\mathcal{L}(\psi, \phi) = \mathbb{E}_{q_\phi(\mathbf{Z}, \mathcal{G}, \Theta)} \left[\log p_\psi(\mathcal{D} \mid \mathbf{Z}, \mathcal{G}, \Theta) - \log \frac{q_\phi(\mathbf{Z}, \mathcal{G}, \Theta)}{p(\mathbf{Z}, \mathcal{G}, \Theta)} \right], \quad (5)$$

where $p(\mathbf{Z}, \mathcal{G}, \Theta)$ is the prior, $p_\psi(\mathcal{D} \mid \mathbf{Z}, \mathcal{G}, \Theta)$ is the likelihood model with parameters ψ , the likelihood model maps the latent variables \mathbf{Z} to high-dimensional vectors \mathbf{X} . An approach to learn this posterior could be to factorize it as

$$q_\phi(\mathbf{Z}, \mathcal{G}, \Theta) = q_\phi(\mathbf{Z}) \cdot q_\phi(\mathcal{G}, \Theta \mid \mathbf{Z}). \quad (6)$$

Given a way to obtain $q_\phi(\mathbf{Z})$, the conditional $q_\phi(\mathcal{G}, \Theta \mid \mathbf{Z})$ can be obtained using existing Bayesian structure learning methods. Otherwise, one has to perform a hard simultaneous optimization which

would require alternating optimizations on \mathbf{Z} and on (\mathcal{G}, Θ) given an estimate of \mathbf{Z} . Difficulty of such an alternate optimization is discussed in [Brehmer et al. \(2022\)](#).

Alternate factorization of the posterior: Rather than factorizing as in equation 6, we propose to factorize according to the BN in figure 3. This is given by $q_\phi(\mathbf{Z}, \mathcal{G}, \Theta) = q_\phi(\mathbf{Z} | \mathcal{G}, \Theta) \cdot q_\phi(\mathcal{G}, \Theta)$. The advantage of this factorization is that the distribution over \mathbf{Z} is completely determined from the SCM given (\mathcal{G}, Θ) and exogenous noise variables (assumed to be Gaussian). Thus, the prior $p(\mathbf{Z} | \mathcal{G}, \Theta)$ and the posterior $p(\mathbf{Z} | \mathcal{G}, \Theta, \mathcal{D}) = q_\phi(\mathbf{Z} | \mathcal{G}, \Theta)$ are identical. This conveniently avoids the hard simultaneous optimization problem mentioned above since optimizing for $q_\phi(\mathbf{Z})$ is not necessary. Equation 5 can then be simplified as

$$\mathcal{L}(\psi, \phi) = \mathbb{E}_{q_\phi(\mathbf{Z}, \mathcal{G}, \Theta)} \left[\log p_\psi(\mathcal{D} | \mathbf{Z}) - \log \frac{q_\phi(\mathcal{G}, \Theta)}{p(\mathcal{G}, \Theta)} - \log \frac{q_\phi(\mathbf{Z} | \mathcal{G}, \Theta)}{p(\mathbf{Z} | \mathcal{G}, \Theta)} \right]. \quad (7)$$

Such a posterior can be used to obtain an SCM by sampling \mathcal{G} and Θ from the approximated posterior. As long as the samples \mathcal{G} are always acyclic, one can perform ancestral sampling through the SCM to obtain samples corresponding to the causal variables $\hat{\mathbf{z}}^{(i)}$. For additive noise models like in equation 2, these samples are already reparameterized and differentiable with respect to their parameters. The samples of causal variables are then fed to the likelihood model to predict $\hat{\mathbf{x}}^{(i)}$ to reconstruct the observed data $\mathbf{x}^{(i)}$.

4.3 POSTERIOR PARAMETERIZATIONS AND PRIORS

For linear Gaussian latent SCMs, which is the focus of this work, learning a posterior over (\mathcal{G}, Θ) is equivalent to learning $q_\phi(W, \Sigma)$ – a posterior over weighted adjacency matrices W and noise covariances Σ . We follow an approach similar to [\(Cundy et al., 2021\)](#). We express W via a permutation matrix P^1 and a lower triangular edge weight matrix L , according to $W = P^T L^T P$. Here, L is defined in the space of all weighted adjacency matrices with a fixed node ordering where node j can be a parent of node i only if $j > i$. Search over permutations corresponds to search over different node orderings and thus, W and Σ parameterize the space of SCMs. Further, we factorize the approximate posterior $q_\phi(P, L, \Sigma)$ as

$$q_\phi(\mathcal{G}, \Theta) \equiv q_\phi(W, \Sigma) \equiv q_\phi(P, L, \Sigma) = q_\phi(P | L, \Sigma) \cdot q_\phi(L, \Sigma). \quad (8)$$

Combining equation 7 and 8 leads to the following ELBO which has to be maximized (derived in [A.1](#)), and the overall algorithm for Bayesian latent causal discovery is summarized in algorithm 1,

$$\mathcal{L}(\psi, \phi) = \mathbb{E}_{q_\phi(L, \Sigma)} \left[\mathbb{E}_{q_\phi(P | L, \Sigma)} \left[\mathbb{E}_{q_\phi(\mathbf{Z} | P, L, \Sigma)} [\log p_\psi(\mathcal{D} | \mathbf{Z})] - \log \frac{q_\phi(P | L, \Sigma)}{p(P)} \right] - \log \frac{q_\phi(L, \Sigma)}{p(L)p(\Sigma)} \right]. \quad (9)$$

Distribution over (L, Σ) : The posterior distribution $q_\phi(L, \Sigma)$ has $\binom{d(d-1)}{2} + 1$ elements to be learnt in the equal noise variance setting. This is parameterized as a diagonal covariance normal distribution. For the prior $p(L)$ over the edge weights, we promote sparse DAGs by using a horseshoe prior [\(Carvalho et al., 2009\)](#), similar to [Cundy et al. \(2021\)](#). A Gaussian prior is defined over log Σ .

Distribution over P : Since the values of P are discrete, performing a discrete optimization is combinatorial and becomes quickly intractable with increasing d . This can be handled by relaxing the discrete permutation learning problem to a continuous optimization problem. This is commonly done by introducing a Gumbel-Sinkhorn [\(Mena et al., 2018\)](#) distribution and where one has to calculate $S((T + \gamma)/\tau)$, where T is the parameter of the Gumbel-Sinkhorn, γ is a matrix of standard Gumbel noise, and τ is a temperature parameter. The logits T are predicted by passing the predicted (L, Σ) through an MLP. In the limit of infinite iterations and as $\tau \rightarrow 0$, sampling from the distribution returns a doubly stochastic matrix. During the forward pass, a hard permutation P is obtained by using the Hungarian algorithm [\(Kuhn, 1955\)](#) which allows $\tau \rightarrow 0$. During the backward pass, a soft permutation is used to calculate gradients similar to [\(Cundy et al., 2021; Charpentier et al., 2022\)](#). We use a uniform prior $p(P)$ over permutations.

¹A permutation matrix $P \in \{0, 1\}^{d \times d}$ is a bistochastic matrix with $\sum_i p_{ij} = 1 \forall j$ and $\sum_j p_{ij} = 1 \forall i$.

Algorithm 1 Bayesian latent causal discovery to learn $\mathcal{G}, \Theta, \mathbf{Z}$ from high dimensional data

Input: \mathcal{D}, \mathcal{I}

Output: $\mathcal{G}, \Theta, \mathbf{Z}$

- 1: Initialize $q_\phi(L, \Sigma)$, $\text{MLP}_{\phi(T)}$, $p_\psi(\mathbf{X} | \mathbf{Z})$, τ and set learning rate α
- 2: **for** num_epochs **do**
- 3: $(\widehat{L}, \widehat{\Sigma}) \sim q_\phi(L, \Sigma)$
- 4: $T \leftarrow \text{MLP}_{\phi(T)}(\widehat{L}, \widehat{\Sigma})$ ▷ Compute logits for sampling from $q_\phi(P | L, \Sigma)$
- 5: $\gamma \in \mathbb{R}^{d \times d} \sim \text{standard Gumbel}$
- 6: $\widehat{P}_{\text{soft}} \leftarrow \text{Sinkhorn}((T + \gamma)/\tau)$
- 7: $\widehat{P}_{\text{hard}} \leftarrow \text{Hungarian}(\widehat{P}_{\text{soft}})$
- 8: $\widehat{W} \leftarrow \widehat{P}^T \widehat{L}^T \widehat{P}$
- 9: **for** $i \leftarrow 1$ to N **do**
- 10: $\mathcal{C}^{(i)} \leftarrow \text{argwhere}(\mathcal{I}^{(i)} = 1)$
- 11: $\widetilde{W} = \text{copy}(\widehat{W})$
- 12: $\widetilde{W}[:, \mathcal{C}^{(i)}] \leftarrow 0$ ▷ Mutated weighted adjacency matrix according to $\mathcal{I}^{(i)}$
- 13: $\widetilde{W}_{\mathcal{I}^{(i)}} \leftarrow \widetilde{W}$
- 14: $\hat{\mathbf{z}}^{(i)} \leftarrow \text{AncestralSample}(\widetilde{W}_{\mathcal{I}^{(i)}}, \widehat{\Sigma})$
- 15: **end for**
- 16: $\hat{\mathbf{Z}} \leftarrow \{\hat{\mathbf{z}}^{(i)}\}_{i=1}^N$
- 17: $\widehat{\mathcal{D}} \sim p_\psi(\mathbf{X} | \mathbf{Z})$
- 18: $\psi \leftarrow \psi + \alpha \cdot \nabla_\psi(\mathcal{L}(\psi, \phi))$ ▷ Update network parameters
- 19: $\phi \leftarrow \phi + \alpha \cdot \nabla_\phi(\mathcal{L}(\psi, \phi))$
- 20: **end for**
- 21: **return** binary(\widehat{W}), ($\widehat{W}, \widehat{\Sigma}$), $\hat{\mathbf{Z}}$

5 EXPERIMENTS AND EVALUATION

We perform experiments to evaluate the learned $(\mathbf{Z}, \mathcal{G}, \Theta)$ of the true linear Gaussian latent SCM from high-dimensional data. We aim to highlight the performance of our proposed method on latent causal discovery. As proper evaluation in such a setting would require access to the GT causal graph that generated the high-dimensional observations, we test our method against baselines on synthetically generated vector data and in the realistic case of learning the SCM from pixels in the chemistry environment dataset of (Ke et al., 2021), both of which have a GT causal structure to be compared with. Further, we evaluate the ability of our model to sample images from unseen interventional distributions.

Baselines: Since we are, to the best of our knowledge, the first to study this setting of learning latent SCMs from low level observations, we are not aware of baseline methods that solve this task. However, we compare our approach against two baselines: (i) Against VAE that has a marginal independence assumption between latent variables and thus have a predefined structure in the latent space, and (ii) against GraphVAE (He et al., 2019) that learns a structure between latent variables. For all baselines, we treat the learned latent variables as causal variables and compare the recovered structure, parameters, and causal variables recovered. Since GraphVAE does not learn the parameters, we fix the edge weight over all predicted edges to be 1.

Evaluation metrics: *To evaluate the learned structure*, we use two metrics commonly used in the literature – the expected Structural Hamming Distance (\mathbb{E} -SHD, lower is better) obtains the SHD (number of edge flips, removals, or additions) between the predicted and GT graph and then takes an expectation over SHDs of posterior DAG samples, and the Area Under the Receiver Operating Characteristic curve (AUROC, higher is better) where a score of 0.5 corresponds to a random DAG baseline. *To evaluate the learned parameters* of the linear Gaussian latent SCM, we use the Mean Squared Error (MSE, lower is better) between the true and predicted edge weights. *To evaluate the learned causal variables*, we use the Mean Correlation Coefficient (MCC, higher is better) following Hyvarinen and Morioka (2017); Zimmermann et al. (2021) and Ahuja et al. (2022) which calculates a score between the true and predicted causal variables. See appendix A.3 and A.7 for training curves and more extensive evaluations of the experiments along other metrics. Our results

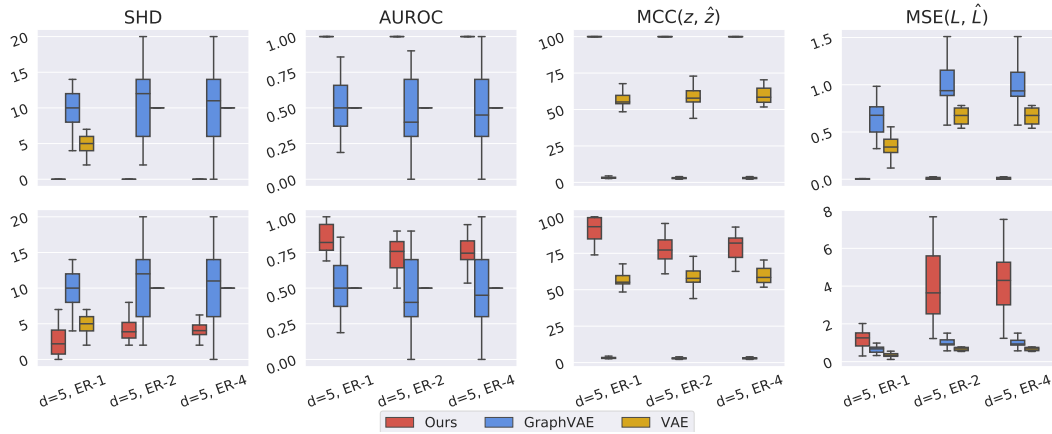


Figure 4: Learning the latent SCM (i) given a node ordering (top) and (ii) over node orderings (bottom) for **linear** projection of causal variables for $d = 5$ nodes, $D = 100$ dimensions: \mathbb{E} -**SHD** (\downarrow), **AUROC** (\uparrow), **MCC** (\uparrow), **MSE** (\downarrow).

are presented over 20 random DAGs with a learning rate of 0.0008. All our implementations are in JAX (Bradbury et al., 2018).

5.1 EXPERIMENTS ON SYNTHETIC DATA

We evaluate our proposed method with the baselines on synthetically generated dataset, where we have complete control over the data generation procedure.

5.1.1 SYNTHETIC VECTOR DATA GENERATION

To generate high-dimensional vector data with a known causal structure, we first generate a random DAG and linear SCM parameters, and generate true causal variables by ancestral sampling. This is then used to generate corresponding high-dimensional dataset with a random projection function.

Generating the DAG and causal variables: Following many works in the literature, we sample random Erdős–Rényi (ER) DAGs (Erdos et al., 1960) with degrees in $\{1, 2, 4\}$ to generate the DAG. For every edge in this DAG, we sample the magnitude of edge weights uniformly as $|L| \sim \mathcal{U}(0.5, 2.0)$ and randomly sample the permutation matrix. We perform ancestral sampling through this random DAG with intervention targets \mathcal{I} , to obtain \mathbf{Z} and then project it to D dimensions to obtain $\{\mathbf{x}^{(i)}\}_{i=1}^N$.

Generating high-dimensional vectors from causal variables: We consider two different cases of generating the high-dimensional data from the causal variables obtained in the previous step: (i) $\mathbf{x}^{(i)}$ is a random linear projection of causal variables, $\mathbf{z}^{(i)}$, from \mathbb{R}^d to \mathbb{R}^D , according to $\mathbf{x} = \mathbf{z}\tilde{P}$, where $\tilde{P} \in \mathbb{R}^{d \times D}$ is a random projection matrix. (ii) $\mathbf{x}^{(i)}$ is a nonlinear projection of causal variables, $\mathbf{z}^{(i)}$, modeled by a 3-layer MLP.

5.1.2 RESULTS ON SYNTHETIC VECTOR DATA

Results on linear projection of causal variables: We present results on the learned causal variables, structure, and parameters in two scenarios: (i) when the true node ordering or permutation is given (e.g., as in He et al. (2019)), and (ii) when the node ordering is *not* given and one has to additionally also infer the permutation P . For $d = 5, 10, 20$ nodes projected to $D = 100$ dimensions, we evaluate our algorithm on synthetic ER-1, ER-2, and ER-4 DAGs. The model was trained for 5000 epochs so as to reach convergence. Figure 4 summarizes the results for $d = 5$ nodes, for which we use 500 observational data points and 2000 interventional data points. Of the 2000 interventional data, we generate 100 random interventional data points per set over 20 intervention sets². It can be seen that when permutation is given, the proposed method can recover the causal graph correctly

²An intervention set is defined as a set of nodes on which an intervention is performed

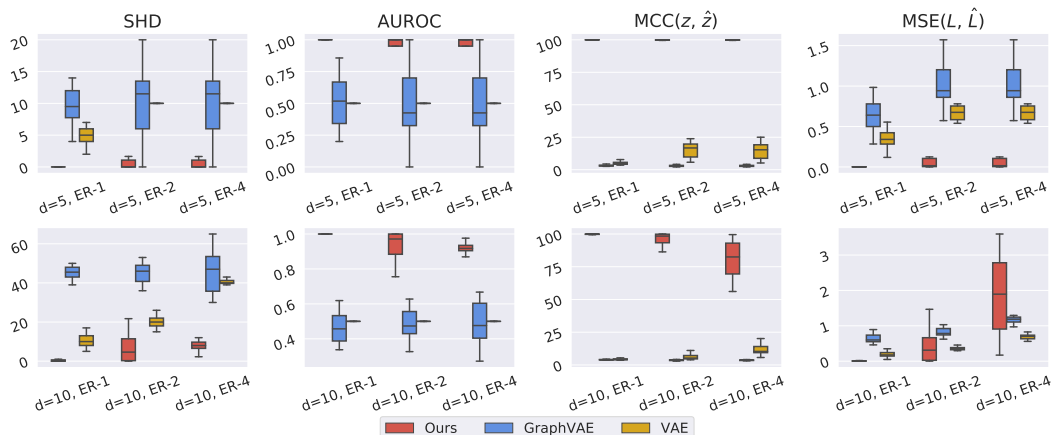


Figure 5: Learning the latent SCM for **nonlinear** projection of causal variables for $d = 5$ (top) and $d = 10$ (bottom) nodes, $D = 100$ dimensions. \mathbb{E} -SHD (\downarrow), AUROC (\uparrow), MCC (\uparrow), MSE (\downarrow).

in all the cases, achieving \mathbb{E} -SHD of 0 and AUROC of 1. When the permutation is learned, the proposed method still recovers the true causal structure very well. However, this is not the case with baseline methods of VAE and GraphVAE, which perform significantly worse on most of the metrics. Figure 11 and 12 (in Appendix) show the results for $d = 10$ and $d = 20$ nodes.

Results on nonlinear projection of causal variables: For $d = 5, 10, 20$ nodes projected to $D = 100$ dimensions, we evaluate our algorithm on synthetic ER-1, ER-2, and ER-4 DAGs, given the permutation P . Figure 5 summarizes the results for 5 and 10 nodes. As in the linear case, the proposed method recovers the true causal structure and the true causal variables, and is significantly better than the VAE and GraphVAE baselines on all the metrics considered. For experiments in this setting, we noticed empirically that learning the permutation is hard, and performs not so different from a null graph baseline (Figure 13). This observation works that theoretically show the identifiability result that recovery of latent variables is possible only upto a permutation in latent causal models (Brehmer et al., 2022; Liu et al., 2022) for general nonlinear mappings between causal variables and low-level data. This supports our observation of not being able to learn the permutation in nonlinear projection settings – but once the permutation is given to the model, it can quickly recover the SCM (figures 5,13). Refer figure 14 (in Appendix) for results on $d = 20$ nodes.

5.2 RESULTS ON LEARNING LATENT SCMS FROM PIXEL DATA

Dataset and Setup: A major challenge with evaluating latent causal discovery models on images is that it is hard to obtain images with corresponding GT graph and parameters. Other works (Kocaoglu et al., 2017; Yang et al., 2021; Shen et al., 2020) handle this by assuming the dataset is generated from certain causal variables (assumed to be attributes like gender, baldness, etc.) and a causal structure that is heuristically set by experts, usually in the CelebA dataset (Liu et al., 2015). This makes evaluation particularly noisy. Given these limitations, we verify if our model can perform latent causal discovery by evaluating on images from the chemistry dataset proposed in Ke et al. (2021) – a scenario where all GT factors are known. We use the environment to generate blocks of different intensities according to a linear Gaussian latent SCM where the parent block colors affect the child block colors then obtain the corresponding images of blocks. The dataset allows generating pixel data from random DAGs and linear SCMs. For this step, we use the same technique to generate causal variables as in the synthetic dataset section.

Results: We perform experiments to evaluate latent causal discovery from pixels and known interventions. The results are summarized in figure 6. It can be seen that the proposed approach can recover the SCM significantly better than the baseline approaches in all the metrics even in the realistic dataset. In figure 7, we also assess the ability of the model to sample images from unseen interventions in the chemistry dataset by examining the generated images with GT interventional samples. The matching intensity of each block corresponds to matching causal variables, which demonstrates model generalization.

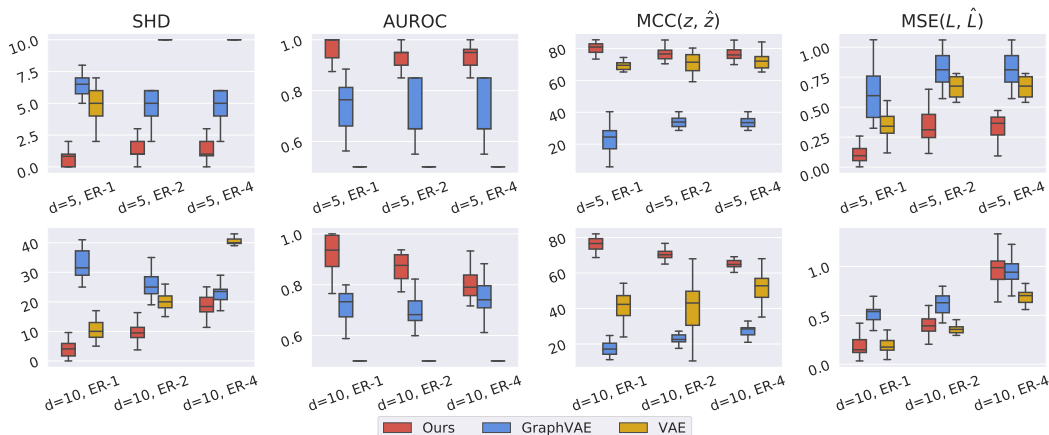


Figure 6: Learning the latent SCM from pixels of the chemistry dataset for $d = 5$ (top) and $d = 10$ nodes (bottom). \mathbb{E} -SHD (\downarrow), AUROC (\uparrow), MCC (\uparrow), MSE (\downarrow)

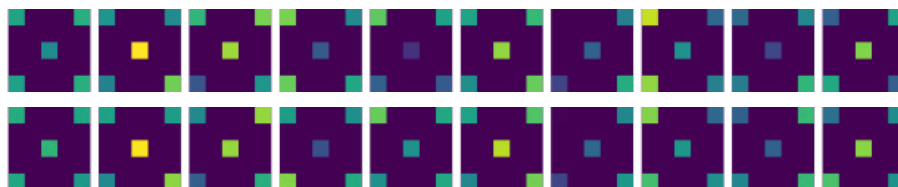


Figure 7: Image sampling from 10 random, unseen interventions: Mean over GT (top row) and predicted (bottom row) image samples in the chemistry dataset for $d = 5$ nodes.

6 CONCLUSION

We presented a tractable approximate inference technique to perform Bayesian latent causal discovery that jointly infers the causal variables, structure and parameters of linear Gaussian latent SCMs under random, known interventions from low-level data. The learned causal model is also shown to generalize to unseen interventions. Our Bayesian formulation allows uncertainty quantification and mutual information estimation which is well-suited for extensions to active causal discovery. Extensions of the proposed method to learn nonlinear, non-Gaussian latent SCMs from unknown interventions would also open doors to general algorithms that can learn causal representations.

7 ACKNOWLEDGEMENTS AND DISCLOSURE OF FUNDING

The authors thank Anirudh Goyal and Sébastien Lachapelle for fruitful discussions and feedback on this work, and to Nanda Harishankar Krishna for reviewing early versions of this paper. We are also thankful to Compute Canada and CIFAR for the compute and funding that made this work possible.

REFERENCES

- Raj Agrawal, Chandler Squires, Karren Yang, Karthikeyan Shanmugam, and Caroline Uhler. Abcd-strategy: Budgeted experimental design for targeted causal structure discovery. In Kamalika Chaudhuri and Masashi Sugiyama, editors, *Proceedings of the Twenty-Second International Conference on Artificial Intelligence and Statistics*, volume 89 of *Proceedings of Machine Learning Research*, pages 3400–3409. PMLR, 16–18 Apr 2019. URL <https://proceedings.mlr.press/v89/agrawal19b.html>.
- Kartik Ahuja, Divyat Mahajan, Vasilis Syrgkanis, and Ioannis Mitliagkas. Towards efficient representation identification in supervised learning, 2022. URL <https://arxiv.org/abs/2204.04606>.

-
- Yashas Annadani, Jonas Rothfuss, Alexandre Lacoste, Nino Scherrer, Anirudh Goyal, Yoshua Bengio, and Stefan Bauer. Variational causal networks: Approximate bayesian inference over causal structures. *arXiv preprint arXiv:2106.07635*, 2021.
- A. Barron, J. Rissanen, and Bin Yu. The minimum description length principle in coding and modeling. *IEEE Transactions on Information Theory*, 44(6):2743–2760, 1998. doi: 10.1109/18.720554.
- Emmanuel Bengio, Moksh Jain, Maksym Korablyov, Doina Precup, and Yoshua Bengio. Flow network based generative models for non-iterative diverse candidate generation. *Advances in Neural Information Processing Systems*, 34:27381–27394, 2021.
- Yoshua Bengio, Aaron Courville, and Pascal Vincent. Representation learning: A review and new perspectives, 2012. URL <https://arxiv.org/abs/1206.5538>.
- Yoshua Bengio, Tristan Deleu, Nasim Rahaman, Rosemary Ke, Sébastien Lachapelle, Olexa Bilaniuk, Anirudh Goyal, and Christopher Pal. A meta-transfer objective for learning to disentangle causal mechanisms, 2019. URL <https://arxiv.org/abs/1901.10912>.
- David M Blei, Alp Kucukelbir, and Jon D McAuliffe. Variational inference: A review for statisticians. *Journal of the American statistical Association*, 112(518):859–877, 2017.
- James Bradbury, Roy Frostig, Peter Hawkins, Matthew James Johnson, Chris Leary, Dougal Maclaurin, George Necula, Adam Paszke, Jake VanderPlas, Skye Wanderman-Milne, et al. Jax: composable transformations of python+ numpy programs. *Version 0.2*, 5:14–24, 2018.
- Johann Brehmer, Pim De Haan, Phillip Lippe, and Taco Cohen. Weakly supervised causal representation learning. *arXiv preprint arXiv:2203.16437*, 2022.
- Philippe Brouillard, Sébastien Lachapelle, Alexandre Lacoste, Simon Lacoste-Julien, and Alexandre Drouin. Differentiable causal discovery from interventional data. *Advances in Neural Information Processing Systems*, 33:21865–21877, 2020.
- Carlos M. Carvalho, Nicholas G. Polson, and James G. Scott. Handling sparsity via the horseshoe. In David van Dyk and Max Welling, editors, *Proceedings of the Twelfth International Conference on Artificial Intelligence and Statistics*, volume 5 of *Proceedings of Machine Learning Research*, pages 73–80, Hilton Clearwater Beach Resort, Clearwater Beach, Florida USA, 16–18 Apr 2009. PMLR. URL <https://proceedings.mlr.press/v5/carvalho09a.html>.
- Bertrand Charpentier, Simon Kibler, and Stephan Günnemann. Differentiable dag sampling. *arXiv preprint arXiv:2203.08509*, 2022.
- Jie Cheng, Russell Greiner, Jonathan Kelly, David Bell, and Weiru Liu. Learning bayesian networks from data: An information-theory based approach. *Artificial Intelligence*, 137(1):43–90, 2002. ISSN 0004-3702. doi: [https://doi.org/10.1016/S0004-3702\(02\)00191-1](https://doi.org/10.1016/S0004-3702(02)00191-1). URL <https://www.sciencedirect.com/science/article/pii/S0004370202001911>.
- David Maxwell Chickering. Optimal structure identification with greedy search. *Journal of machine learning research*, 3(Nov):507–554, 2002.
- Chris Cundy, Aditya Grover, and Stefano Ermon. Bcd nets: Scalable variational approaches for bayesian causal discovery. In M. Ranzato, A. Beygelzimer, Y. Dauphin, P.S. Liang, and J. Wortman Vaughan, editors, *Advances in Neural Information Processing Systems*, volume 34, pages 7095–7110. Curran Associates, Inc., 2021. URL <https://proceedings.neurips.cc/paper/2021/file/39799c18791e8d7eb29704fc5bc04ac8-Paper.pdf>.
- Tristan Deleu, António Góis, Chris Emezue, Mansi Rankawat, Simon Lacoste-Julien, Stefan Bauer, and Yoshua Bengio. Bayesian structure learning with generative flow networks. *arXiv preprint arXiv:2202.13903*, 2022.
- Paul Erdos, Alfréd Rényi, et al. On the evolution of random graphs. *Publ. Math. Inst. Hung. Acad. Sci*, 5(1):17–60, 1960.

-
- Nir Friedman and Daphne Koller. Being bayesian about network structure. *arXiv preprint arXiv:1301.3856*, 2013.
- Dan Geiger and David Heckerman. Learning gaussian networks. In *UAI*, 1994.
- Asish Ghoshal and Jean Honorio. Learning linear structural equation models in polynomial time and sample complexity. In *International Conference on Artificial Intelligence and Statistics*, pages 1466–1475. PMLR, 2018.
- Alexander Hägele, Jonas Rothfuss, Lars Lorch, Vignesh Ram Somnath, Bernhard Schölkopf, and Andreas Krause. Bacadi: Bayesian causal discovery with unknown interventions. *arXiv preprint arXiv:2206.01665*, 2022.
- Jiawei He, Yu Gong, Joseph Marino, Greg Mori, and Andreas Lehrmann. Variational autoencoders with jointly optimized latent dependency structure. In *International Conference on Learning Representations*, 2019. URL <https://openreview.net/forum?id=SJgsCjCqt7>.
- David Heckerman, Dan Geiger, and David M Chickering. Learning bayesian networks: The combination of knowledge and statistical data. *Machine learning*, 20(3):197–243, 1995.
- David Heckerman, Christopher Meek, and Gregory Cooper. A bayesian approach to causal discovery. Technical report, Technical report msr-tr-97-05, Microsoft Research, 1997.
- David Heckerman, Christopher Meek, and Gregory Cooper. A bayesian approach to causal discovery. In *Innovations in Machine Learning*, pages 1–28. Springer, 2006.
- Aapo Hyvarinen and Hiroshi Morioka. Nonlinear ICA of Temporally Dependent Stationary Sources. In Aarti Singh and Jerry Zhu, editors, *Proceedings of the 20th International Conference on Artificial Intelligence and Statistics*, volume 54 of *Proceedings of Machine Learning Research*, pages 460–469. PMLR, 20–22 Apr 2017. URL <https://proceedings.mlr.press/v54/hyvarinen17a.html>.
- Robert E. Kass and Adrian E. Raftery. Bayes factors. *Journal of the American Statistical Association*, 90(430):773–795, 1995. ISSN 01621459. URL <http://www.jstor.org/stable/2291091>.
- Nan Rosemary Ke, Olexa Bilaniuk, Anirudh Goyal, Stefan Bauer, Hugo Larochelle, Bernhard Schölkopf, Michael C Mozer, Chris Pal, and Yoshua Bengio. Learning neural causal models from unknown interventions. *arXiv preprint arXiv:1910.01075*, 2019.
- Nan Rosemary Ke, Aniket Didolkar, Sarthak Mittal, Anirudh Goyal, Guillaume Lajoie, Stefan Bauer, Danilo Rezende, Yoshua Bengio, Michael Mozer, and Christopher Pal. Systematic evaluation of causal discovery in visual model based reinforcement learning. *arXiv preprint arXiv:2107.00848*, 2021.
- Nan Rosemary Ke, Silvia Chiappa, Jane Wang, Jorg Bornschein, Theophane Weber, Anirudh Goyal, Matthew Botvinic, Michael Mozer, and Danilo Jimenez Rezende. Learning to induce causal structure. *arXiv preprint arXiv:2204.04875*, 2022.
- Diederik P Kingma and Max Welling. Auto-encoding variational bayes, 2013. URL <https://arxiv.org/abs/1312.6114>.
- Diederik P. Kingma, Tim Salimans, Rafal Jozefowicz, Xi Chen, Ilya Sutskever, and Max Welling. Improving variational inference with inverse autoregressive flow, 2016. URL <https://arxiv.org/abs/1606.04934>.
- Murat Kocaoglu, Christopher Snyder, Alexandros G. Dimakis, and Sriram Vishwanath. Causalgan: Learning causal implicit generative models with adversarial training, 2017. URL <https://arxiv.org/abs/1709.02023>.
- Mikko Koivisto and Kismat Sood. Exact bayesian structure discovery in bayesian networks. *The Journal of Machine Learning Research*, 5:549–573, 2004.

-
- H. W. Kuhn. The hungarian method for the assignment problem. *Naval Research Logistics Quarterly*, 2(1-2):83–97, 1955. doi: <https://doi.org/10.1002/nav.3800020109>. URL <https://onlinelibrary.wiley.com/doi/abs/10.1002/nav.3800020109>.
- Jack Kuipers, Polina Suter, and Giusi Moffa. Efficient sampling and structure learning of bayesian networks. *Journal of Computational and Graphical Statistics*, pages 1–12, 2022.
- Sébastien Lachapelle, Philippe Brouillard, Tristan Deleu, and Simon Lacoste-Julien. Gradient-based neural dag learning. *arXiv preprint arXiv:1906.02226*, 2019.
- E. L. Lehmann and Joseph P. Romano. *Testing statistical hypotheses*. Springer Texts in Statistics. Springer, New York, third edition, 2005. ISBN 0-387-98864-5.
- Yuke Li, Kenneth Li, Pin Wang, Donglai Wei, Hanspeter Pfister, and Ching-Yao Chan. Intervention-based recurrent causal model for non-stationary video causal discovery, 2022. URL <https://openreview.net/forum?id=JvGzK0lQLet>.
- Phillip Lippe, Sara Magliacane, Sindy Löwe, Yuki M Asano, Taco Cohen, and Stratis Gavves. Citris: Causal identifiability from temporal intervened sequences. In *International Conference on Machine Learning*, pages 13557–13603. PMLR, 2022.
- Yuhang Liu, Zhen Zhang, Dong Gong, Mingming Gong, Biwei Huang, Anton van den Hengel, Kun Zhang, and Javen Qinfeng Shi. Weight-variant latent causal models, 2022. URL <https://arxiv.org/abs/2208.14153>.
- Ziwei Liu, Ping Luo, Xiaogang Wang, and Xiaoou Tang. Deep learning face attributes in the wild. In *Proceedings of the IEEE international conference on computer vision*, pages 3730–3738, 2015.
- David Lopez-Paz and Maxime Oquab. Revisiting classifier two-sample tests, 2016. URL <https://arxiv.org/abs/1610.06545>.
- David Lopez-Paz, Robert Nishihara, Soumith Chintala, Bernhard Schölkopf, and Léon Bottou. Discovering causal signals in images, 2016. URL <https://arxiv.org/abs/1605.08179>.
- Lars Lorch, Jonas Rothfuss, Bernhard Schölkopf, and Andreas Krause. Dibs: Differentiable bayesian structure learning. In M. Ranzato, A. Beygelzimer, Y. Dauphin, P.S. Liang, and J. Wortman Vaughan, editors, *Advances in Neural Information Processing Systems*, volume 34, pages 24111–24123. Curran Associates, Inc., 2021. URL <https://proceedings.neurips.cc/paper/2021/file/ca6ab34959489659f8c3776aaflf8efd-Paper.pdf>.
- Gonzalo Mena, David Belanger, Scott Linderman, and Jasper Snoek. Learning latent permutations with gumbel-sinkhorn networks. *arXiv preprint arXiv:1802.08665*, 2018.
- Raha Moraffah, Bahman Moraffah, Mansooreh Karami, Adrienne Raglin, and Huan Liu. Causal adversarial network for learning conditional and interventional distributions, 2020. URL <https://arxiv.org/abs/2008.11376>.
- Ignavier Ng, AmirEmad Ghassami, and Kun Zhang. On the role of sparsity and dag constraints for learning linear dags. *Advances in Neural Information Processing Systems*, 33:17943–17954, 2020.
- Ignavier Ng, Shengyu Zhu, Zhuangyan Fang, Haoyang Li, Zhitang Chen, and Jun Wang. Masked gradient-based causal structure learning. In *Proceedings of the 2022 SIAM International Conference on Data Mining (SDM)*, pages 424–432. SIAM, 2022.
- Roxana Pamfil, Nisara Sriwattanaworachai, Shaan Desai, Philip Pilgerstorfer, Konstantinos Georgatzis, Paul Beaumont, and Bryon Aragam. Dynotears: Structure learning from time-series data. In *International Conference on Artificial Intelligence and Statistics*, pages 1595–1605. PMLR, 2020.
- Judea Pearl. *Causality*. Cambridge University Press, 2 edition, 2009. doi: 10.1017/CBO9780511803161.

-
- Jonas Peters and Peter Bühlmann. Identifiability of gaussian structural equation models with equal error variances. *Biometrika*, 101(1):219–228, 2014.
- Danilo Jimenez Rezende, Shakir Mohamed, and Daan Wierstra. Stochastic backpropagation and approximate inference in deep generative models, 2014. URL <https://arxiv.org/abs/1401.4082>.
- Nino Scherrer, Olexa Bilaniuk, Yashas Annadani, Anirudh Goyal, Patrick Schwab, Bernhard Schölkopf, Michael C Mozer, Yoshua Bengio, Stefan Bauer, and Nan Rosemary Ke. Learning neural causal models with active interventions. *arXiv preprint arXiv:2109.02429*, 2021.
- Nino Scherrer, Anirudh Goyal, Stefan Bauer, Yoshua Bengio, and Nan Rosemary Ke. On the generalization and adaption performance of causal models, 2022. URL <https://arxiv.org/abs/2206.04620>.
- Bernhard Schölkopf, Dominik Janzing, Jonas Peters, Eleni Sgouritsa, Kun Zhang, and Joris Mooij. On causal and anticausal learning, 2012. URL <https://arxiv.org/abs/1206.6471>.
- Bernhard Schölkopf, Francesco Locatello, Stefan Bauer, Nan Rosemary Ke, Nal Kalchbrenner, Anirudh Goyal, and Yoshua Bengio. Towards causal representation learning, 2021. URL <https://arxiv.org/abs/2102.11107>.
- Xinwei Shen, Furu Liu, Hanze Dong, Qing Lian, Zhitang Chen, and Tong Zhang. Disentangled generative causal representation learning, 2020. URL <https://arxiv.org/abs/2010.02637>.
- Shohei Shimizu, Takanori Inazumi, Yasuhiro Sogawa, Aapo Hyvärinen, Yoshinobu Kawahara, Takashi Washio, Patrik O Hoyer, and Kenneth Bollen. Directlingam: A direct method for learning a linear non-gaussian structural equation model. *The Journal of Machine Learning Research*, 12: 1225–1248, 2011.
- P. Spirtes, C. Glymour, and R. Scheines. *Causation, Prediction, and Search*. MIT press, 2nd edition, 2000.
- Casper Kaae Sønderby, Tapani Raiko, Lars Maaløe, Søren Kaae Sønderby, and Ole Winther. Ladder variational autoencoders, 2016. URL <https://arxiv.org/abs/1602.02282>.
- Panagiotis Tigas, Yashas Annadani, Andrew Jesson, Bernhard Schölkopf, Yarin Gal, and Stefan Bauer. Interventions, where and how? experimental design for causal models at scale. *arXiv preprint arXiv:2203.02016*, 2022.
- Christian Toth, Lars Lorch, Christian Knoll, Andreas Krause, Franz Pernkopf, Robert Peharz, and Julius von Kügelgen. Active bayesian causal inference. *arXiv preprint arXiv:2206.02063*, 2022.
- Ashish Vaswani, Noam Shazeer, Niki Parmar, Jakob Uszkoreit, Llion Jones, Aidan N Gomez, Łukasz Kaiser, and Illia Polosukhin. Attention is all you need. *Advances in neural information processing systems*, 30, 2017.
- Jussi Viinikka, Antti Hyttinen, Johan Pensar, and Mikko Koivisto. Towards scalable bayesian learning of causal dags. *Advances in Neural Information Processing Systems*, 33:6584–6594, 2020.
- Benjie Wang, Matthew R Wicker, and Marta Kwiatkowska. Tractable uncertainty for structure learning. In *International Conference on Machine Learning*, pages 23131–23150. PMLR, 2022.
- Yixin Wang and Michael I. Jordan. Desiderata for representation learning: A causal perspective, 2021. URL <https://arxiv.org/abs/2109.03795>.
- Dennis Wei, Tian Gao, and Yue Yu. Dags with no fears: A closer look at continuous optimization for learning bayesian networks. *Advances in Neural Information Processing Systems*, 33:3895–3906, 2020.

- Feng Xie, Biwei Huang, Zhengming Chen, Yangbo He, Zhi Geng, and Kun Zhang. Identification of linear non-Gaussian latent hierarchical structure. In Kamalika Chaudhuri, Stefanie Jegelka, Le Song, Csaba Szepesvari, Gang Niu, and Sivan Sabato, editors, *Proceedings of the 39th International Conference on Machine Learning*, volume 162 of *Proceedings of Machine Learning Research*, pages 24370–24387. PMLR, 17–23 Jul 2022. URL <https://proceedings.mlr.press/v162/xie22a.html>.
- Mengyue Yang, Furui Liu, Zhitang Chen, Xinwei Shen, Jianye Hao, and Jun Wang. Causalvae: Disentangled representation learning via neural structural causal models. In *Proceedings of the IEEE/CVF Conference on Computer Vision and Pattern Recognition*, pages 9593–9602, 2021.
- Yue Yu, Jie Chen, Tian Gao, and Mo Yu. Dag-gnn: Dag structure learning with graph neural networks. In *International Conference on Machine Learning*, pages 7154–7163. PMLR, 2019.
- Yue Yu, Tian Gao, Naiyu Yin, and Qiang Ji. Dags with no curl: An efficient dag structure learning approach, 2021. URL <https://arxiv.org/abs/2106.07197>.
- Zhen Zhang, Ignavier Ng, Dong Gong, Yuhang Liu, Ehsan M Abbasnejad, Mingming Gong, Kun Zhang, and Javen Qinfeng Shi. Truncated matrix power iteration for differentiable dag learning, 2022. URL <https://arxiv.org/abs/2208.14571>.
- Shengjia Zhao, Jiaming Song, and Stefano Ermon. Learning hierarchical features from deep generative models. In Doina Precup and Yee Whye Teh, editors, *Proceedings of the 34th International Conference on Machine Learning*, volume 70 of *Proceedings of Machine Learning Research*, pages 4091–4099. PMLR, 06–11 Aug 2017. URL <https://proceedings.mlr.press/v70/zhao17c.html>.
- Xun Zheng, Bryon Aragam, Pradeep K Ravikumar, and Eric P Xing. Dags with no tears: Continuous optimization for structure learning. *Advances in Neural Information Processing Systems*, 31, 2018.
- Roland S. Zimmermann, Yash Sharma, Steffen Schneider, Matthias Bethge, and Wieland Brendel. Contrastive learning inverts the data generating process, 2021. URL <https://arxiv.org/abs/2102.08850>.

A APPENDIX

A.1 DERIVATION OF THE ELBO

From equation 7, we want to minimize the KL divergence between the true and approximate posteriors:

$$\begin{aligned}
& D_{\text{KL}}(q_\phi(\mathbf{Z}, \mathcal{G}, \Theta) \parallel p(\mathbf{Z}, \mathcal{G}, \Theta \mid \mathcal{D})) \\
&= -\mathbb{E}_{(\mathbf{z}, \mathcal{g}, \Theta) \sim q_\phi(\mathbf{z}, \mathcal{g}, \Theta)} \left[\log p(\mathcal{D} \mid \mathbf{z}, \mathcal{g}, \Theta) - \log \frac{q_\phi(\mathcal{G}, \Theta)}{p(\mathcal{G}, \Theta)} \right] + \log p(\mathcal{D}) \\
&= -\mathbb{E}_{(\mathcal{g}, \Theta) \sim q_\phi(\mathcal{G}, \Theta)} \left[\mathbb{E}_{\mathbf{z} \sim q_\phi(\mathbf{z} \mid \mathcal{g}, \Theta)} [\log p(\mathcal{D} \mid \mathbf{z})] - \log \frac{q_\phi(\mathcal{G}, \Theta)}{p(\mathcal{G}, \Theta)} \right] + \log p(\mathcal{D}) \\
&= -\mathbb{E}_{(P, L, \Sigma) \sim q_\phi(P, L, \Sigma)} \left[\mathbb{E}_{\mathbf{z} \sim q_\phi(\mathbf{z} \mid P, L, \Sigma)} [\log p(\mathcal{D} \mid \mathbf{z})] - \log \frac{q_\phi(P, L, \Sigma)}{p(P, L, \Sigma)} \right] + \log p(\mathcal{D}) \\
& \hspace{20em} \text{(from 8)} \\
&= -\mathbb{E}_{(L, \Sigma) \sim q_\phi(L, \Sigma)} \left[\mathbb{E}_{P \sim q_\phi(P \mid L, \Sigma)} \left[\mathbb{E}_{\mathbf{z} \sim q_\phi(\mathbf{z} \mid P, L, \Sigma)} [\log p(\mathcal{D} \mid \mathbf{z})] - \log \frac{q_\phi(P \mid L, \Sigma)}{p(P)} \right] \right. \\
& \quad \left. - \log \frac{q_\phi(L, \Sigma)}{p(L)p(\Sigma)} \right] + \log p(\mathcal{D}) \hspace{2em} \text{(via the factorization in 8)}
\end{aligned}$$

Since the log evidence $\log p(\mathcal{D})$ is a constant, minimizing the KL divergence corresponds to maximizing the following ELBO:

$$\max \mathbb{E}_{(L, \Sigma) \sim q_\phi(L, \Sigma)} \left[\mathbb{E}_{P \sim q_\phi(P|L, \Sigma)} \left[\mathbb{E}_{\mathbf{Z} \sim q_\phi(\mathbf{Z}|P, L, \Sigma)} [\log p(\mathcal{D} | \mathbf{Z})] - \log \frac{q_\phi(P | L, \Sigma)}{p(P)} \right] - \log \frac{q_\phi(L, \Sigma)}{p(L)p(\Sigma)} \right]$$

A.2 IMPLEMENTATION DETAILS

A.3 TRAINING CURVES

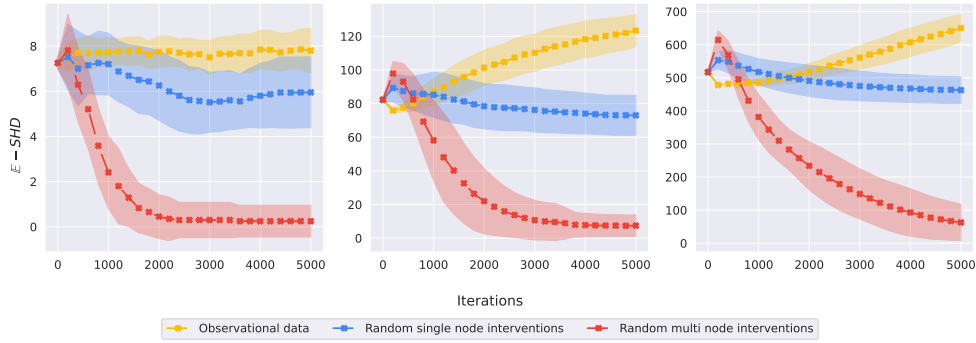


Figure 8: Learning latent SCM parameters given a fixed node ordering for linearly projected causal variables for random ER-1 DAGs with $d = 6, 20, 50$ nodes. The model was trained for 5000 iterations over 3500 data samples out of which 500 were observational points for the single and multi node intervention runs.

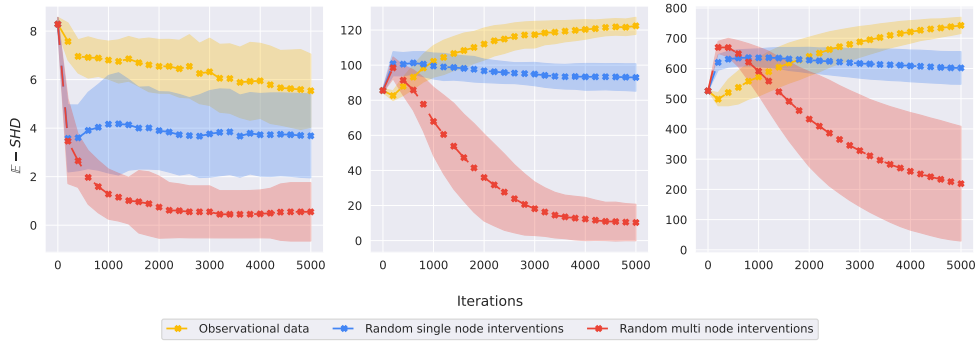


Figure 9: Learning latent SCM parameters given a fixed node ordering for linearly projected causal variables for random ER-2 DAGs with $d = 6, 20, 50$ nodes. The model was trained for 5000 iterations over 3500 data samples out of which 500 were observational points for the single and multi node intervention runs.

A.4 LINEAR PROJECTION EXPERIMENTS

Details for figure 11, $d = 10$ nodes: The dataset consists of 500 observational points and 20000 interventional points. To sample the 20000 interventional points, we randomly choose 200 intervention sets, and for each intervention set we sample 100 data points. The model was trained for 8000 epochs to reach convergence.

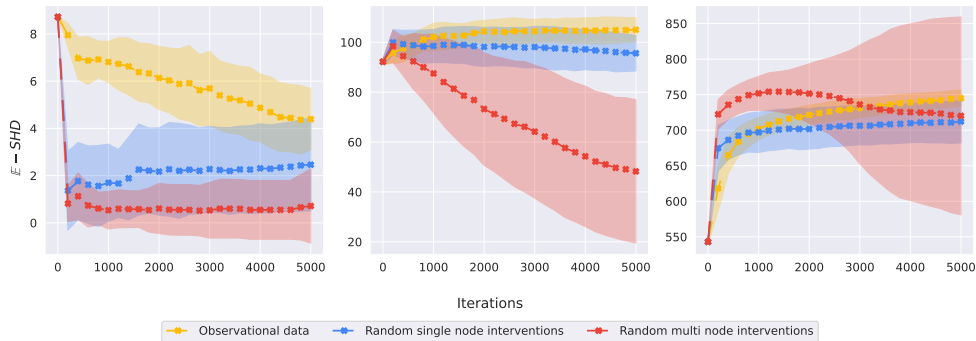


Figure 10: Learning latent SCM parameters given a fixed node ordering for linearly projected causal variables for random ER-4 DAGs with $d = 6, 20, 50$ nodes. The model was trained for 5000 iterations over 3500 data samples out of which 500 were observational points for the single and multi node intervention runs.

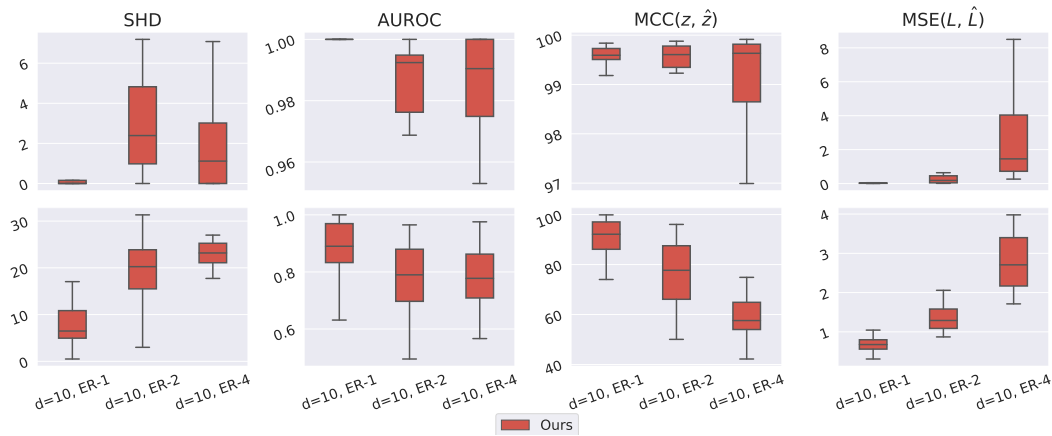


Figure 11: Learning the latent SCM (i) given a node ordering (top) and (ii) over node orderings (bottom) for **linear** projection of causal variables for $d = 10$ nodes, $D = 100$ dimensions.

Details for figure 12, $d = 20$ nodes: The dataset consists of 500 observational points and 20000 interventional points. To sample the 20000 interventional points, we randomly choose 100 intervention sets, and for each intervention set we sample 200 data points. The model was trained for 3000 epochs to reach convergence.

A.5 NONLINEAR PROJECTION EXPERIMENTS

Figure 13 contains the results for the latent causal discovery problem with and without learning a permutation. Figure 14 shows the results for 500 observational samples and 10000 interventional samples with 100 intervention sets and 100 samples per set on $d = 20$ nodes and $D = 100$ dimensions.

A.6 ABLATION STUDY: EFFECT OF PERFORMANCE WITH RESPECT TO NUMBER OF INTERVENTION TYPES

Here, we study how the performance and recovery of the latent SCM is affected with respect to the number of intervention types in the dataset. The number of intervention types refers to different combinations of nodes we perform interventions on. For all experiments in this subsection, we use 100 interventional samples per type of intervention. Figure 15 and 16 show results on vector data where the high-dimensional vector is a linear projection of the causal variables. Figure 17 and 18

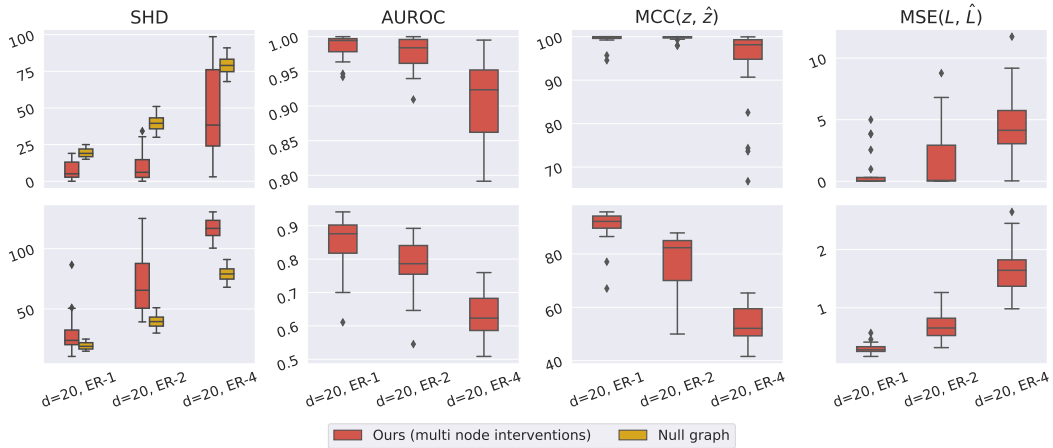


Figure 12: Learning the latent SCM (i) given a node ordering (top) and (ii) over node orderings (bottom) for **linear** projection of causal variables for $d = 20$ nodes, $D = 100$ dimensions.

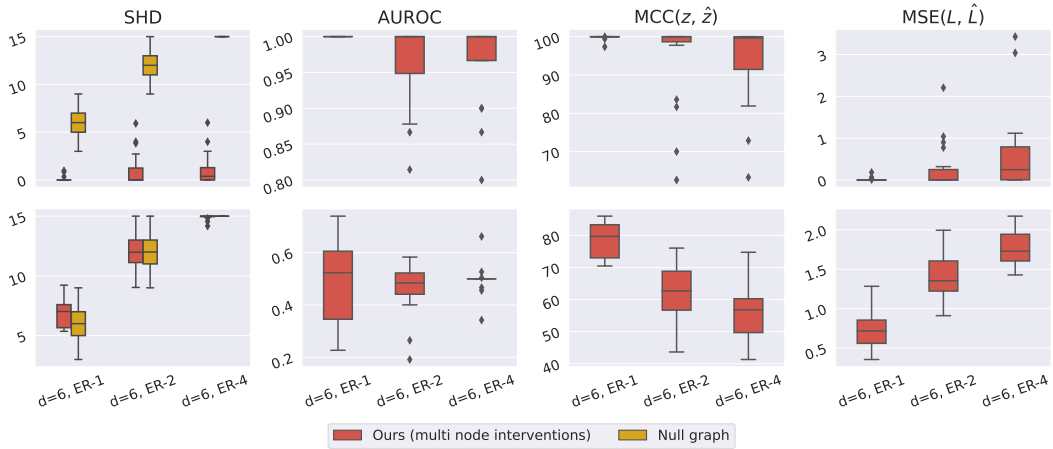


Figure 13: Learning the latent SCM (i) given a node ordering (top) and (ii) over node orderings (bottom) for **nonlinear** projection of causal variables for $d = 6$ nodes, $D = 100$ dimensions.

summarize results on vector data where the high-dimensional vector is a nonlinear projection of the causal variables.

A.7 COMPLETE EVALUATION

For the experiments already presented in the main text, this section contains additional a more comprehensive evaluation on the following metrics:

- **SHD_C**: The expected CPDAG SHD between the GT and predicted DAG's skeletons.
- **SHD**: The expected SHD between the GT and predicted DAG.
- **MCC**: The expected Mean Correlation Coefficient between the predicted and true causal variables.
- **AUROC** between predicted and true graph structure.
- **FPR**: False positive rate
- **FN**: False negative
- **TP**: True positive

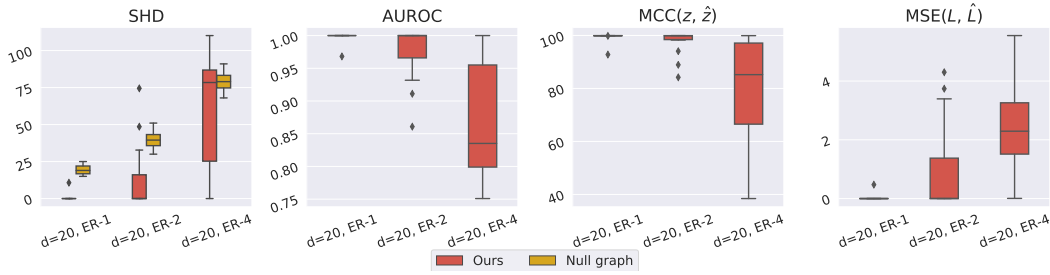


Figure 14: Learning the latent SCM given a node ordering for **nonlinear** projection of causal variables for $d = 20$ nodes, $D = 100$ dimensions.

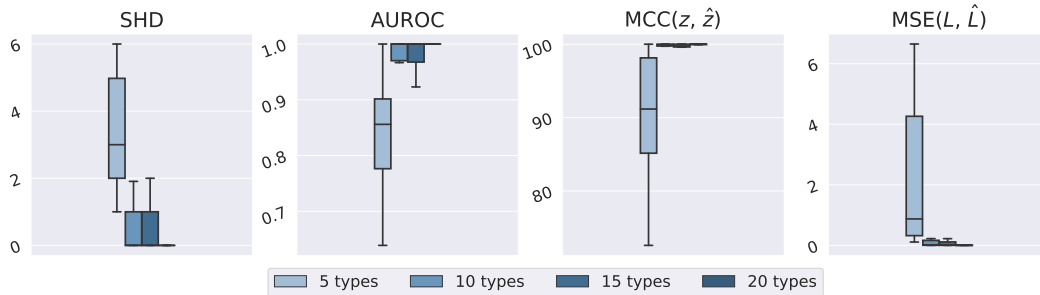


Figure 15: Effect of number of intervention types seen versus on the performance of learning the latent SCM given a node ordering for $d = 5$ nodes, $D = 100$ dimensions.

- **AUPRC_G**: Area under precision-recall curves
- **Precision** of the graph structure prediction
- **TN**: True negatives
- **FP**: False positives
- **TPR**: True positive rate
- **Recall** of the graph structure prediction
- **AUPRC_W**:
- **F1 Score** = $2 * Precision * Recall / (Precision + Recall)$
- **L_MSE**: Mean squared error between predicted and true edge weights.
- **X_MSE**: Mean squared reconstruction error over the high dimensional (low-level) data
- **true_obs_KL_term_Z**: The KL divergence between the predicted and GT observational joint distributions.

Figure 19 shows the complete evaluation on 18 different metrics for $d = 5$ nodes. The dataset consists of 500 observational points and 2000 interventional points. To sample the 2000 interventional points, we randomly choose 20 intervention sets, and for each intervention set we sample 100 data points with random intervention values.

A.8 ADDITIONAL RELATED WORK

Causal discovery and structure learning: [Annadani et al. \(2021\)](#) casts the Bayesian structure learning problem as an autoregressive one by sequentially predicting edges, in hopes of capturing the potentially multi-modal posterior. [Deleu et al. \(2022\)](#) uses Generative Flow Networks, or GFlowNets ([Bengio et al., 2021](#)), a new class of probabilistic methods that lies at the intersection of reinforcement learning and variational inference. The work uses the transitive closure property ensuring that the action space is constrained to actions that do not introduce cycles. [Chickering \(2002\)](#) proposes a greedy search algorithm, but does not scale to large number of nodes. [Wang et al. \(2022\)](#) leverages sum product networks to perform exact Bayesian structure learning. [Hägele](#)

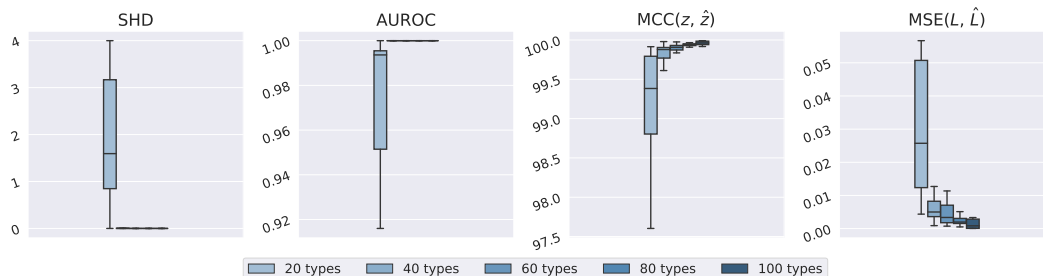


Figure 16: Effect of number of intervention types seen versus on the performance of learning the latent SCM given a node ordering for $d = 10$ nodes, $D = 100$ dimensions.

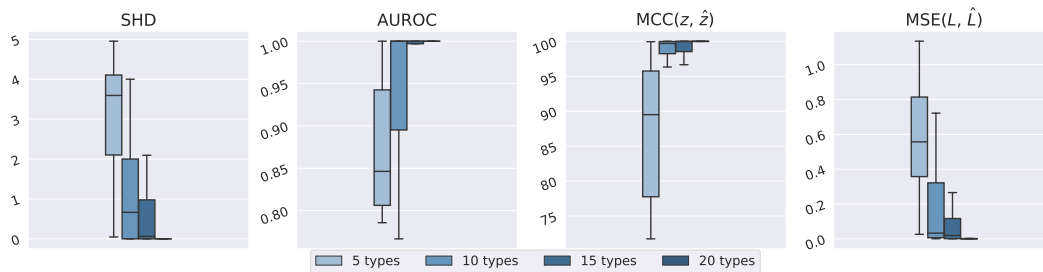


Figure 17: Ablation: effect of number of intervention types seen versus on the performance of learning the latent SCM given a node ordering for $d = 5$ nodes, $D = 100$ dimensions.

[et al. \(2022\)](#) extends the framework of [Lorch et al. \(2021\)](#) to perform Bayesian causal discovery in a setting where interventions are unknown. [Xie et al. \(2022\)](#) is in a setting where the edges exist not just between latent causal variables but with high-dimensional variables in the dataset as well. Other efforts include ([Shimizu et al., 2011](#); [Lopez-Paz and Oquab, 2016](#); [Yu et al., 2019](#); [Ghoshal and Honorio, 2018](#); [Ng et al., 2020](#); [Li et al., 2022](#)).

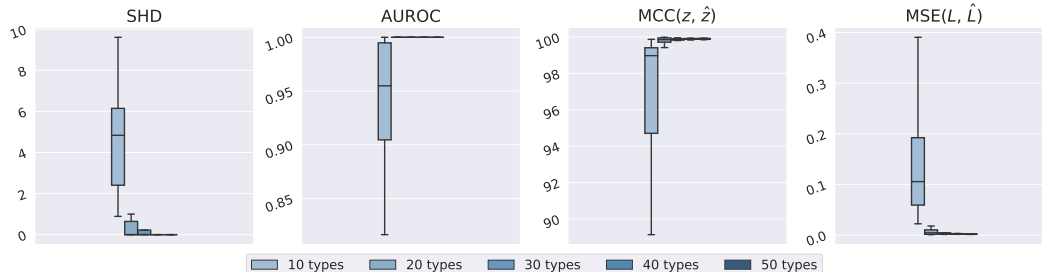


Figure 18: Ablation: effect of number of intervention types seen versus on the performance of learning the latent SCM given a node ordering for $d = 10$ nodes, $D = 100$ dimensions.

Table 1: Average experiment runtimes

Nodes (d)	Dataset size	Experiment	Projection	Steps	Avg. runtime (min)
5	2500	Vector data	Linear (fixed ordering)	5000	12
10	10500	Vector data	Linear (fixed ordering)	3000	25
10	10500	Vector data	Linear (learned ordering)	3000	90
20	80500	Vector data	Linear (fixed ordering)	3000	150
20	20500	Vector data	Linear (learned ordering)	3000	360
20	80500	Vector data	Linear (learned ordering)	8000	540
10	5500	Vector data	Nonlinear	2000	12
5	2500	Vector data	Nonlinear	5000	15
20	10500	Vector data	Nonlinear	10000	100
5	2500	Image data	Nonlinear	2000	40
5	5500	Image data	Nonlinear	2000	75
10	2500	Image data	Nonlinear	2000	50
10	5500	Image data	Nonlinear	2000	80

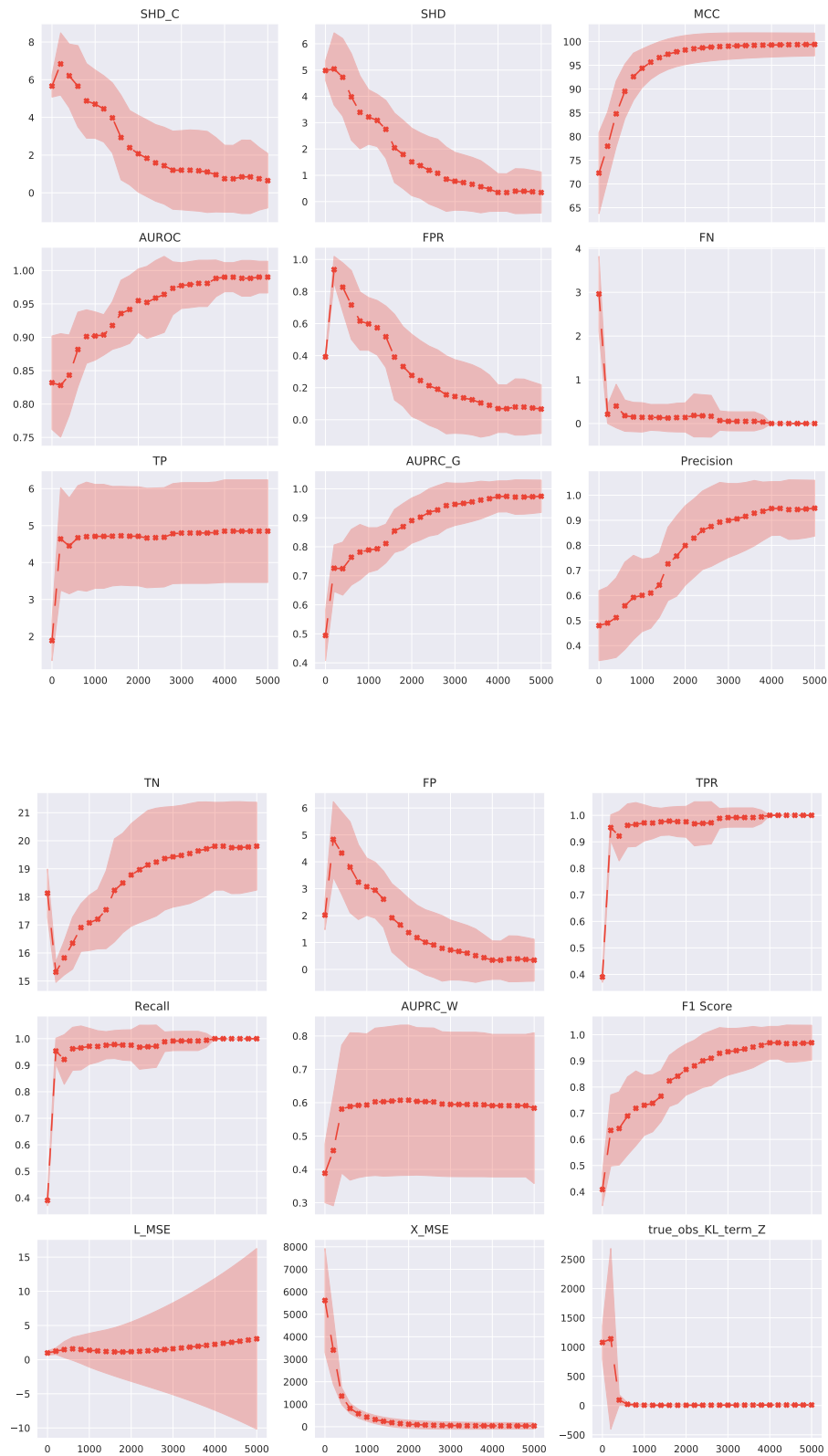


Figure 19: Training curves: Metric versus number of iterations for $d = 5$ nodes linearly projected to $D = 100$ dimensions, with 20 intervention sets, 100 interventional samples per intervention set, and 500 observational samples.